PAH and OPAH Flux during the Deepwater Horizon Incident

Lane G. Tidwell, **Sarah E. Allan**, **Steven G. O'Connell**, **Kevin A. Hobbie**, **Brian W. Smith**, and **Kim A. Anderson**[*]

Environmental and Molecular Toxicology Department, Oregon State University, ALS 1007, Corvallis, OR 97331

Abstract

Passive sampling devices were used to measure air vapor and water dissolved phase concentrations of 33 polycyclic aromatic hydrocarbons (PAHs) and 22 oxygenated PAHs (OPAHs) at four Gulf of Mexico coastal sites prior to, during and after shoreline oiling from the Deepwater Horizon oil spill (DWH). Measurements were taken at each site over a 13 month period, and flux across the water-air boundary was determined. This is the first report of vapor phase and diffusive flux of both PAHs and OPAHs during the DWH. Vapor phase sum PAH and OPAH concentrations ranged between 6.6 and 210 ng/m^3 and 0.02 and 34 ng/m^3 respectively. PAH and OPAH concentrations in air exhibited different spatial and temporal trends than in water, and air-water flux of 13 individual PAHs was shown to be at least partially influenced by the DWH incident. The largest PAH volatilizations occurred at the sites in Alabama and Mississippi at nominal rates of 56,000 and 42,000 ng/m^2/day in the summer. Naphthalene was the PAH with the highest observed volatilization rate of 52,000 ng/m^2/day in June 2010. This work represents additional evidence of the DWH incident contributing to air contamination, and provides one of the first quantitative air-water chemical flux determinations with passive sampling technology.

Keywords

Mississippi canyon block 252; low density polyethylene; diffusive sampling; environmental disaster

Introduction

The explosion of the Deepwater Horizon (DWH) oil rig on April 20th 2010 led to the release of approximately 4.1 million gallons of oil into the Gulf of Mexico.[1] Between April 28 and July 19, 411 *in situ* burns were undertaken to remove oil from the water surface.[2] An additional non-mechanical response included the application of 2.1 million gallons of chemical dispersants at the wellhead and to off-shore surface waters which likely increased the freely dissolved fraction of the oil constituents.[3-4] Crude oil released from the Macondo 252 well during the DWH incident contained an estimated 3.9% of polycyclic aromatic

hydrocarbons (PAHs) by weight.[5] PAHs are chemicals of concern in oil, and their fate and transport in the environment is an important component of understanding potential impacts from spills.

While PAHs have been widely studied for many decades, oxygenated polycyclic aromatic hydrocarbons (OPAHs) are an emerging contaminant of concern. Interest in OPAHs has increased in the last decade due to their presence in the environment coupled with the toxicity of some OPAHs.[6-7] Individual OPAHs consist of one or more oxygen atoms attached to an aromatic ring structure that may also contain other chemical groups.[8] Formation of these compounds through both biotic and abiotic mechanisms could be expected during the DWH incident especially, through photo-oxidation of PAHs in air and waters.[6, 9]

Low-density polyethylene (LDPE) passive sampling devices (PSDs) have been used in water and air to assess time-integrated environmental concentrations of many dissolved and vapor phase contaminants respectively, including PAHs and OPAHs.[10-12] Air sampling is often focused on determining the concentration of particulate bound chemicals; however, exposure to the PAH vapor phase has been shown to account for up to 86% of the cancer-risk from inhalation exposure. [13-15] Vapor phase PAHs are by definition unbound to particulates which means this atmospheric fraction is respirable and bioavailable. Similarly, the dissolved fraction of contaminants in water is bioavailable for passive uptake by organisms.[10, 16] In addition to being biologically relevant, the gas phase and dissolved concentrations of chemicals are the fractions that flux from one environmental compartment to another. [17-19]

PSDs are ideally suited for flux measurements since they specifically sequester the dissolved water phase and air vapor phase fractions. Generally, great effort is required to acquire the dissolved water fraction including multiple filtration steps and solid phase cleanup(s).[20] Additionally, the filtered water is only operationally defined as dissolved, as any particles smaller than the filter are also extracted. The PSDs employed are not subject to filter bias due to their lipophilic carbon polymer design and average pore size of 10 angstroms that characterize diffusion samplers.[11] Until recently, investigation of flux using PSDs has only assessed the overall direction of flux based on the air water partition compound coefficients (K_{aw}), or through concentration gradients measured in both air and water samples.[21-22] To the authors' knowledge there are only two reports of measuring the actual magnitude of PAH flux using PSDs, and a separate investigation of flux targeting a different chemical class.[23-25]

The air-water flux of PAHs is an important factor in understanding the fate of spilled oil.[26] Though air and water quality monitoring were conducted during the DWH oil spill, no studies to the authors' knowledge have reported on flux of PAHs and OPAHs across the air-water boundary. In this study, we present the air vapor phase PAH and OPAHs at coastal sites in Louisiana, Mississippi, Alabama and Florida prior to, during and after shoreline oiling. Spatial and temporal trends for individual PAHs and OPAHs were examined during 13 months. We also address the data gap of aromatic hydrocarbon flux during episodic events. Using PSDs for quantitative flux assessment is a developing technological

advancement in environmental chemistry, and this work is the first to quantitatively measure flux during an environmental disaster.

Correction to Original Article

This article is a corrected form of Tidwell *et al*, which was originally published in 2015, DOI: 10.1021/es503827y.[27] Vapor phase PAH and OPAH measured concentrations in air were corrected, as were the air-water flux mass exchange rates. Corrections were made due to the detection of an honest calculation error found in the original manuscript. Errors resulted from using incorrect units of the ideal gas constant and improper cell linkages in the spreadsheet that was used to adjust air concentrations for sampling temperature. The original article was retracted by the authors.[28] This version of the article presents corrected versions of all of the original analyses and discussions.

Materials and Methods

Sample collection

Sampling was performed at four coastal sites: Grand Isle, Louisiana (LA); Gulfport, Mississippi (MS); Gulf Shores, Alabama (AL); and Gulf Breeze, Florida (FL) (Figure 1A, 1B). Air and water samples were collected concurrently during twelve sampling events from May 2010 to June 2011, sampling durations for flux assessment ranged from 3 to 41 days (see Supporting Information (SI) Table 1 for specific dates).[16]

Stainless steel air sampler cages that allowed for air circulation while minimizing sampler exposure to water, particulate depositions, and UV (Figure 1C) were deployed concurrently with water cages described previously.[16] A total of five PSDs were deployed in each air or water cage. Air samplers were located between 1-5 m above the water surface and were directly above water samplers.[16] Approximately one meter long PSDs were constructed from LDPE tubing, and were fortified with deuterated PAH performance reference compounds (PRCs) for water or air sampling rate calculations. A list of PRCs can be found in SI List 1. PRCs spanned a range of K_{oa}/K_{ow}s similar to the target analyte PAHs and OPAHs, and the most similar PRC was used for quantification (SI List 1). OPAHs were quantified using PAH PRCs, any biases generated from this approach are conservative since PAHs have slightly higher K_{oa}/K_{ow}s than the analogous OPAHs.[29-32] Detailed PSD conditioning, construction, clean up and extraction is described in Anderson *et al.,* 2008.[33] PSDs were transported in sealed polytetrafluoroethylene (PTFE) air-tight bags. Samples were stored in the laboratory at 4°C until extraction within two weeks of receipt.

Sample processing and chemical analysis

All solvents used were Optima® grade or better (Fisher Scientific, Pittsburg, PA), and standards were purchased at purities ≥ 97%. All five PSDs from each cage were extracted as a composite representing a single sample in order to increase analytic sensitivity. PAH and OPAH in PSDs were extracted by dialysis with n-hexane detailed in Anderson *et al.,* 2008[33], use of n-hexane for extraction of OPAH is explained in O'Connell *et al.,* 2014.[34] Extracts were stored in amber glass vials at -20°C until instrumental analysis.

PAH and OPAH analysis used an Agilent 5975B Gas Chromatograph-Mass Spectrometer (GC-MS) with an Agilent DB-5MS column (30m × 0.25mm × 0.25μm) in electron impact mode (70 eV) using selective ion monitoring (SIM). PAH GC parameters are detailed in Allan *et al.,* 2012[16], and OPAH parameters are detailed in O'Connell *et al.,* 2013.[35] Six and nine point calibration curves for PAHs and OPAHs respectively had correlation coefficients > 0.98 for all target analytes, a list of measured analytes are in SI (Lists 1-2).

Quality control

Quality control (QC) samples accounted for over 30% of the total number of samples analyzed and included: PSD construction blanks, field and trip blanks for each deployment and retrieval, post-deployment cleaning blanks and laboratory reagent blanks. Extraction surrogates were added to all samples immediately prior to extraction and concentrations were surrogate corrected. All compounds were below detection limits in all blank QC samples. Mean extraction surrogate recoveries were 52.5% (range 37-113) for naphthalene-D8, 67.8% (range 53–116) for acenaphthylene-D8, 80.1% (range 77–113) phenanthrene-D10, 97.8% (84-118) fluoranthene-D10, 105% (86-139) for chrysene-D12, 80.5% (68-90) benzo(a)pyrene-D12, 66.7% (50-85) for dibenzo(g,h,i)perylene-D12, 66% (44-80) for 1,4-naphthalenequnione-D8, 104% (80-140) for 9-flourenone-D8, and 96% (60-150) for 9,10-anthraquinone-D8.

Air-water flux calculation

Environmental vapor concentrations were determined using an empirical uptake model with sampling rates derived by measuring PRC loss as described by Huckins *et al.,* 2006 and others.[11,29, 31, 36] Details and formulas are presented in SI. Previously published water concentrations were used for calculation of PAH flux and are described in detail in Allan *et al.,* 2012.[16]

The exchange of chemicals between air and water at the interface can be described as the movement of a chemical from the bulk phase, followed by transport across the thin films of each phase into the receiving compartment. The Whitman two film model is used to calculate this movement:

$$F = K_{ol}\left(C_w - \frac{c_a}{H_{T'}}\right) \quad \text{Eq. 1}$$

where F is the flux (ng/m^2 day^{-1}), the total mass-transfer rate coefficient is K_{ol} (m/day), and C_w and C_a are the dissolved and vapor phase concentrations in the water and air respectively. [17-18] H_T', in this case, is a compound-specific temperature-corrected Henry's law value. A unitless Henry's law value can be calculated using equation 2:

$$H' = \frac{H}{RT} \quad \text{Eq. 2}$$

where R is the ideal gas constant (8.2057×10^{-5} m^3 atm K^{-1} mol^{-1}) and T is the temperature in Kelvin. Air and water temperatures were collected hourly using temperature loggers co-located with PSDs at each sampling site the average temperature over each deployment was calculated and used for assessment of the temperature corrected Henry's law values. The temperature correction for H' to yield H$_T$' in equation 1 is calculated using equation 3:

$$H_{T'} = H'_{(298)} \times e^{\frac{\Delta H_{vap}}{R} \times \left(\frac{1}{T} - \frac{1}{298} \right)} \quad \text{Eq. 3}$$

where T is the temperature in Kelvin, $H vap$ is the compound specific enthalpy of vaporization, and R is the ideal gas constant for the compound (R in kJ*K^{-1}*mol^{-1}). The total mass transfer coefficient in Eq. 1 can be calculated according to equation 4:

$$\frac{1}{K_{ol}} = \frac{1}{k_a H'} + \frac{1}{k_w} \quad \text{Eq. 4}$$

where k_a is the air side mass transfer coefficient and k_w is the water side mass transfer coefficient. Average wind speed over the course of the deployment was calculated from NOAA data published on the tides and currents web interface.[37] Published diffusivity values for 13 PAHs were used to calculate Schmidt values as inputs for mass transfer coefficients.[38] An estimate of OPAH flux was performed on 7 OPAHs, using PAH analogue diffusivity values, and are considered semi-quantitative as a result. Details of the calculations are further described in Johnson 2010 and Bamford *et al.,* 1999.[39, 18] Flux was only assessed when the compound was detected in both environmental compartments. PSD concentrations represent a time weighted average concentration, therefore the net flux for each sampling period is the time weighted average flux over the sampling duration. Using PSDs to assess the time weighted flux provides an alternative new way to characterize movement of chemicals over a time period. PSD flux is especially well suited to applications where episodic changes and releases are important to capture and characterize. Assigning additional uncertainties to mass transfer coefficients derived from average values was determined to be an overly conservative approach. As a result, the error bars present on the flux figures in Figure 2 and Figure 4 represent the pooled variance of the flux from an n=12 replication study performed in the Gulf of Mexico during this study.

Data modeling

Differences between sites and between sampling times were assessed using Wilcoxon rank-sum tests, and differences were considered significant at a probability value of p 0.05. Confidence intervals were calculated from a Gulf of Mexico air and water replication study performed using n=12 PSDs and represents the pooled variance.[40] The average percent difference between sum PAH replicates in water and air at each site were 18 and 41 respectively. Principal component analysis (PCA) was used to explore changes in chemical profiles of samples; a specific description can be found in SI. Analytes in the PCA below

instrumental detection limits were assigned a value of one half the limit of environmental detection, information on detection limits can be found in SI Table 3.

Results and Discussion

Vapor PAHs in coastal air of four Gulf Coast states

Prior to shoreline oiling at LA, the measured Σ_{33air} PAH at this site was 29.9 ($\pm$13) ng/m^3. This decreased to 8.67 ($\pm$3.8) ng/m^3 the following month when there was visible shoreline oiling (Figure 2A). The June-1 sampling event was significantly greater (p 0.05) than the June 2 sampling event. Σ_{33air} PAH concentrations tended to increase earlier than PAH concentrations in water (Figure 2B from Allan $et\ al.$ 2012[16]), which could be due to faster atmospheric transport, as well as contributions from in-$situ$ burn events.[41-42]

At MS, the June-1 Σ_{33air} PAH was significantly higher than all other sampling times ($p <$ 0.05), methylated naphthalene's comprised over 90% of the Σ_{33air} PAH in June-1. Although Middlebrook $et\ al.$ 2012 did not measure PAHs (except naphthalene) their bulk organic carbon measurements, taken at concurrent time points with the June-1 sampling, are consistent with our high Σ_{33air} PAH, providing converging lines of evidence that the DWH incident had tangible impacts on near shore Gulf of Mexico air.[43]

The temporal trend of bioavailable PAHs at the AL site was different than MS but has a similar profile as the LA site (Figure 2A). The Σ_{33air}PAH concentration was highest in September at 48.2 ($\pm$14) ng/m^3. The highest observed $\Sigma_{33water}$PAH was in September at 25 ($\pm$2) ng/m^3.[16] High wind events and continued near-shore clean-up activities were observed during those sampling periods (SI Table 2) and the air PAH trend observed is consistent with a re-circulation/suspension of contaminated waters/sediments and some volatilization. Other possible explanations include increased local inputs such as marine traffic or other oil sources.

The coastal air at FL had an initial Σ_{33air} PAH concentration of 26.1 ($\pm$14) ng/m^3. A trend of increasing Σ_{33air}PAH from May 2010 through August was observed, but was not statistically different from other sampling periods ($p = 0.1$). The FL Σ_{33air} PAH are similar in concentration to those observed in LA in May 2010 and June-1.

All sites taken together displayed a temporal pattern of increases in the maximum air PAH concentrations occurring earlier at the western sites and later in the eastern locations. This could be explained by the distance of the sites from the wellhead, in addition to $in\ situ$ burns and air currents in the Gulf of Mexico.[43-44] The site at MS was most heavily impacted in June 2010. A similar trend was observed in water samples.[16] Dispersion and aging of oil and oil chemicals could also explain this trend; if DWH is a primary source of PAHs during this time period, then a decrease of vapor phase PAH would be expected.[45-46]

Comparing Gulf of Mexico air PAHs to literature values

The vapor phase Σ_{33air}PAH concentrations in this study ranged between 6 and 210 ng/m^3, and are comparable to PAH concentrations reported at rural and coastal metropolitan regions, but are significantly less than PAH concentrations found in large cities. For instance

the vapor phase Σ_{13}PAH concentrations of 3.06 and 24.1 ng/m^3 recorded in the coastal metropolitan region of Kozani and the rural region of Petrana, Greece respectively give an example of coastal regions that have similar population densities as the sampling sites in this study but that have relatively smaller PAH concentrations.[47] A 2006 study near a petroleum industry harbor in Belgium found Σ_{16}PAH vapor phase concentrations to range between 15 and 135 ng/m^3 during different seasons, overlapping with the measured PAHs in this study.[48] Conversely, very high vapor phase concentrations were observed in the inland metropolitan region of Alexandria Egypt, with Σ_{42}PAH concentrations ranging between 390 and 990 ng/m^3.[49] The highest individual PAH contributions to the total PAH load in this study were naphthalene, phenanthrene and 2-methyl phenanthrene (SI Figure S1,S2), which are similar to other studies of vapor phase PAHs at petroleum impacted sites or areas of moderate urbanization.[47-48]

PAH air-water exchange

Predicting the fate of PAHs during environmental disasters includes characterizing the exchange of PAHs across the air-water boundary.[18, 20] While many fate models for the DWH oil spill assumed volatilization was an important transfer and fate mechanism, this pathway has not been directly quantified.[26] Air-water exchange (flux) of 13 PAHs was determined at the four sites over a 13 month period that spanned the DWH incident (Figure 2C-E). Σ_{13}PAH net flux was positive at 39 out of 44 time points; meaning volatilization of PAHs from the water to the air. The greatest Σ_{13}PAH net flux to air occurred at MS and AL, observed during July at 56,200 ($\pm$17,100) ng/m^2/day, and August at 42,900 ($\pm$17,000) ng/m^2/day, respectively.

The Σ_{13}PAH flux to air peaked at LA in August, at 15,300 ($\pm$14,900) ng/m^2/day. After the DWH *in situ* burns stopped and the well head was capped, the Σ_{13}PAH flux decreases at LA, MS and FL sites. Interestingly, six months after the peakΣ_{13}PAH flux volatilization was about 5 -fold lower at the LA site, but flux of PAHs from water to air was still 1.7 -fold greater than observed in May 2010 prior to shoreline oiling. This may be due to the continuing influence of DWH oil in this area.

Individual PAHs showed more variability in flux direction and magnitude than the net PAH flux. The greatest volatilization at MS and AL was naphthalene at 52,200 ($\pm$2,600) and 27,500 ($\pm$1000) ng/m^2/day during the June-2 sampling event. The second largest individual PAH volatilization at LA was phenanthrene at 10,500 ($\pm$10,200) ng/m^2/day in June-1 and the largest deposition was -265 ($\pm$240) ng/m^2/day in May 2010. The shift of flux from deposition to volatilization for phenanthrene is an important indicator of increased dissolved PAH levels in water rather than decreased vapor phase PAH levels in air. In 1999, Bamford *et al.*, found that local inputs from an urban setting to surface waters resulted in similar degassing events, indicating that local sources such as industrial activities, or an oil spill in this case, may strongly influence the flux of PAHs.[18] Naphthalene underwent the largest observed single PAH deposition events at MS and AL at a rates of -6000 ($\pm$300) ng/m^2/day in April and -3900 ($\pm$150) ng/m^2/day in February respectively (Figure 2E).

Few other relevant studies are available for comparison of individual PAHs, but a study in a heavily industrialized harbor in Taiwan showed phenanthrene to be undergoing deposition

during 19 of the 22 sampling time points.[19] Additionally, another study reported the observed mean annual flux of phenanthrene along the southern coastline of Singapore to be -457 (±490) ng/m2/day. [50] A third investigation shows phenanthrene in deposition phase for all but one observation in Lake Erie and Lake Ontario,[23] and a fourth investigation of PAH flux found phenanthrene to be in or near equilibrium for all sites with detectable levels of phenanthrene in both air and water.[25] All of these studies illustrate that the typical trend for phenanthrene is deposition under many environmental conditions, however, we found during the DWH incident along the coast of the Gulf of Mexico phenanthrene was volatizing. The change from deposition to volatilization of phenanthrene at LA, MS and FL sites give strength to the supposition that the influx of hydrocarbons from the DWH incident changed the direction of phenanthrene flux well after visible oil was gone. The AL site did not shift from deposition to volatilization as observed at the other three sites and does not exhibit the characteristic phenanthrene deposition observed in other flux investigations.[19, 23, 50] However, there was an increase in volatilization later in the study showing that a perturbation of the steady state flux at this site occurred. Continuous volatilization of phenanthrene at AL might be explained by the local marine and residential activities which were in close proximity. The proximity of residential and marine activity at AL may have introduced phenanthrene directly to the water through runoff or marine engine use and maintenance. Sources such as local residences and other anthropogenic activities have been shown to affect PAH air-water dynamics.[18, 23]

PAH chemical profiles and source modeling

Principle component analysis (PCA) using air data in profile form was used to produce score and loading plots, shown in Figure 3A. The two score plots differ only by the choice of deployment time or state labels. PCA was also performed on individual state air data, as seen in Figure 3B. The score plots show some delineation between pre-cap and post-cap samples, with pre-cap samples being grouped tightly to one another and on the periphery of the majority of the post-cap samples. An exception to this is the earliest post-cap sample (#4) in each state which groups further away from both the pre-cap and all other post-cap samples. As the sampling progressed after the DWH incident, the proportion of p1 (naphthalene) increases from time point 5-10 (August-April). Furthermore, post-cap sampling events 5-11 (August-May2011) show less intra-sample variation than pre-cap observations 1-3 (May2010-June-2), suggesting the homogeneity of post-cap samples consistent with a single episodic event impacting pre-cap samples Figure 3A-B.

Figure 3C shows source ratios enriched in 2- and 3-ring PAHs compared to 4- to 6-ring PAHs in May and June-1 at all sites, consistent with a petrogenic source.[51-52] Ratios with values greater than 1 are indicative of a petrogenic source.[52] The alkylated-PAH versus parent PAH profiles are dominantly also petrogenic in June-1 at LA and MS, see SI Figure S2 for alkylation profiles. In urban environments, no single source was expected; this was consistent with our observations of mixed alkylated profiles observed later in 2010 and 2011.

Oxygenated polycyclic aromatic hydrocarbons in air and water

Few OPAH concentrations in air and water have been quantified using PSDs.[35] Oxygenated hydrocarbons were reported during the DWH incident using active sampling techniques; however, the specific oxygenated analytes were not identified.[53] OPAHs detected in DWH crude oil were identified in both water and air samples (SI Table 4). During this study 11 OPAHs were quantified, five of those OPAHs were detected in most of the samples (SI-Figure S3). The most abundant OPAHs in air during the DWH incident were acenaphthenequinone, benzofluorenone, 9,10-anthraquinone, and 9-fluorenone (Figures 2A-C and SI S3). Over the course of the study, the OPAH with the highest concentrations in water were phenanthrene-1,4-dione, and acenaphthenequinone in LA, MS and AL while 1,4-anthraquinone was the largest contribution in water at FL (SI Figure S3). Sum OPAHs at LA peaked in June-2 in air and June-1 in water, Σ_{22air}OPAH 17 ($\pm$1) ng/m^3 and $\Sigma_{22water}$OPAH 635 ($\pm$60) ng/L. The individual OPAHs contributing to this high Σ_{22air} OPAH were chromone and acenaphthenequinone, after the June-2 sample, a decrease of 10-15 fold was observed in Σ_{22air}OPAH concentrations. However, water concentrations of phenanthrene-1,4-dione 257 ($\pm$40) ng/L, and acenaphthenequinone 185 ($\pm$30) ng/L remained elevated at LA through May 2011.

$\Sigma_{22water}$OPAH concentrations at the MS site were less than 25 ng/L for the first six sampling periods (Figure 2C). The most frequently observed was benzofluorenone (SI Figure S3). $\Sigma_{22water}$OPAH concentrations were elevated in February, April and May 2011 at concentrations of 369 ($\pm$60), 262 ($\pm$40), and 112 ($\pm$20) ng/L respectively, $p < 0.05$ when compared to the other 5 sampling events for each of these observations. In each instance, acenaphthenequinone had the greatest contribution to the $\Sigma_{22water}$OPAH. Conversely, Σ_{22air}OPAH at MS was significantly higher in May 2011 at 1.1 ($\pm$0.05) ng/m^3 than in all previous sampling times (p 0.05). The high concentrations of OPAHs in air in May 2011 suggest that air quality may have been impacted by factors other than the DWH incident, given the proximity of this site to urban and industrial activities, it is important to consider possible inputs from local sources. Increased levels of OPAHs in Gulf of Mexico waters during later sampling in 2011 may be evidence of the continuing transformation of PAHs in the system into OPAHs.

The Σ_{22air}OPAH levels at AL were approximately 200-fold less than the highest concentrations observed at LA or FL. The highest Σ_{22air}OPAH at AL was during June-2 sampling at 0.18 ($\pm$0.1) ng/m^3, and concentrations gradually decreased throughout the study to a minimum of 3.4E-3 ($\pm$2.8E-3) ng/m^3 in April (Figure 4A). OPAHs in water were minimal at the onset of sampling and peaked during the last sampling event. The lowest $\Sigma_{22water}$OPAH concentration at AL, 2.2 ($\pm$0.5), was observed during May 2010 and the highest $\Sigma_{22water}$OPAH, 617 ($\pm$100) ng/L, was recorded during May 2011.

The highest concentration Σ_{22air}OPAH observed during the study was measured at FL in July at level of 34 ($\pm$1.8) ng/m^3; this observation was significantly different from all other samples ($p < 0.05$) (Figure 4A). The high concentration is largely due to chromone (SI Figure S3). Due to short atmospheric half-lives and multiple formation pathways, positively identifying sources of OPAH is an ongoing research question. The potential for July Σ_{22air}OPAH at this site to be affected by factors other than DWH is likely. $\Sigma_{22water}$OPAH

concentrations in FL reached a peak concentration of 92 (±50) in June-1 a value nominally six times lower than the highest observed concentration at the LA site (Figure 4C). Unlike the other three sites, waterborne OPAH in Gulf Breeze, FL showed little temporal variation during the course of this research.

In a study in southern France, the highest combined gas and particle OPAH values observed was nominally 50 to 70% less than the highest concentrations observed in LA and FL respectively.[54] The high concentrations of vapor phase OPAHs observed during July is much higher than what has been previously characterized in typical urban settings.[54] A study in Texas showed elevated vapor phase levels of benz[a]anthracene-7,12-dione during the summer, and was proposed to be a result of temperature dependent partitioning between the particle bound and vapor phase OPAHs.[55] While similar meteorological conditions occurred during this study, the OPAH levels actually decreased dramatically during the summer. This observation lends support to the idea that elevated levels were due to a specific input(s) disrupting typical environmental conditions, and not simply a shift in partitioning between the vapor and aerosol phase.[56-58] A study performed in Oregon on the Willamette River in the Portland Harbor Superfund found dissolved OPAH concentrations in water ranging from 6 ng/L to 50 ng/L.[34] This observation by O'Connell *et al.* 2014 is nominally 12 times lower than the highest water value reported here.[34] While toxicity of OPAHs is not thoroughly known, early evidence suggest development toxicity may be the same or higher for some OPAHs than the parent PAH.[7] Therefore, OPAHs appear to be an important consideration as part of the transport, weathering and ecosystem health during environmental disasters.[9, 53]

OPAH air-water exchange

To the authors' knowledge this is the first report of OPAH flux. Direction and approximate magnitude for the OPAH flux is show in Figure 4D-F. Structures of the OPAHs investigated in this flux assessment can be found in SI figure S4. Unlike PAHs, where the net flux changed from volatilization to deposition during the study, Σ_7OPAH flux was in volatilization at all sites throughout the study. LA and AL had the largest magnitude of volatilization in June-1 and August, respectively. Large Σ_7OPAH volatilization at all four sites was primarily driven by the movement of acenaphthenequinone and benzofluoreneone from water to air. Benzofluorenone flux at each site was of significantly lower magnitude than acenaphthenequinone; however, benzofluorenone was found to be of a very transient nature, with decreasing rates of volatilization over time in LA and FL and large spikes in volatilization in September in MS and LA. . The nature of the dynamic movement between environmental compartments and the observed magnitudes indicate further investigation of OPAH flux is warranted. The extremely high magnitude of OPAH flux to the atmosphere concurrent with the DWH incident shows that OPAHs as well as PAHs need to be assessed for environmental fate and transport when assessing the long term impacts of an environmental disaster.

Supplementary Material

Refer to Web version on PubMed Central for supplementary material.

Acknowledgments

References

1. Camilli R, Di Iorio D, Bowen A, Reddy CM, Techet AH, Yoerger DR, Whitcomb LL, Seewald JS, Sylva SP, Fenwick J. Acoustic measurement of the Deepwater Horizosn Macondo well flow rate. Proceedings of the National Academy of Sciences. 2012; 109(50):20235–20239.

2. Aurell, J. Aerostat sampling of PCDD/PCDF emissions from the Gulf oil spill in situ burns. DIANE Publishing; 2010.

3. Kujawinski EB, Kido Soule MC, Valentine DL, Boysen AK, Longnecker K, Redmond MC. Fate of dispersants associated with the Deepwater Horizon oil spill. Environmental Science & Technology. 2011; 45(4):1298–1306. [PubMed: 21265576]

4. NRC., N. R. C. O. S. B.. Oil Spill Dispersants: Efficacy and Effects. National Acadamy of Sciences; 2005.

5. Reddy CM, Arey JS, Seewald JS, Sylva SP, Lemkau KL, Nelson RK, Carmichael CA, McIntyre CP, Fenwick J, Ventura GT. Composition and fate of gas and oil released to the water column during the Deepwater Horizon oil spill. Proceedings of the National Academy of Sciences. 2012; 109(50): 20229–20234.

6. Lundstedt S, White PA, Lemieux CL, Lynes KD, Lambert LB, Oberg L, Haglund P, Tysklind M. Sources, fate, and toxic hazards of oxygenated polycyclic aromatic hydrocarbons (PAHs) at PAH-contaminated sites. Ambio. 2007; 36(6):475–485. [PubMed: 17985702]

7. Knecht AL, Goodale BC, Truong L, Simonich MT, Swanson AJ, Matzke MM, Anderson KA, Waters KM, Tanguay RL. Comparative developmental toxicity of environmentally relevant oxygenated PAHs. Toxicology and applied pharmacology. 2013; 271(2):266–275. [PubMed: 23684558]

8. Wischmann H, Steinhart H. The formation of PAH oxidation products in soils and soil/compost mixtures. Chemosphere. 1997; 35(8):1681–1698.

9. Layshock JA, Wilson G, Anderson KA. Ketone and quinone-substituted polycyclic aromatic hydrocarbons in mussel tissue, sediment, urban dust, and diesel particulate matrices. Environmental Toxicology and Chemistry. 2010; 29(11):2450–2460. [PubMed: 20830751]

10. Sower GJ, Anderson KA. Spatial and temporal variation of freely dissolved polycyclic aromatic hydrocarbons in an urban river undergoing superfund remediation. Environmental Science & Technology. 2008; 42(24):9065–9071. [PubMed: 19174872]

11. Huckins, JN.; Petty, JD.; Booij, K. Monitors of organic chemicals in the environment: semipermeable membrane devices. Springer; New York: 2006.

12. O'Connell SG, Haigh T, Wilson G, Anderson KA. An analytical investigation of 24 oxygenated-PAHs (OPAHs) using liquid and gas chromatography–mass spectrometry. Analytical and bioanalytical chemistry. 2013; 405(27):8885–8896. [PubMed: 24005604]

13. Ramírez N, Cuadras A, Rovira E, Marcé RM, Borrull F. Risk assessment related to atmospheric polycyclic aromatic hydrocarbons in gas and particle phases near industrial sites. Environmental health perspectives. 2011; 119(8):1110. [PubMed: 21478082]

14. Tsai PJ, Shieh HY, Lee WJ, Lai SO. Characterization of PAHs in the atmosphere of carbon black manufacturing workplaces. Journal of hazardous materials. 2002; 91(1):25–42. [PubMed: 11900904]

15. Liu Y, Tao S, Dou H, Zhang T, Zhang X, Dawson R. Exposure of traffic police to polycyclic aromatic hydrocarbons in Beijing, China. Chemosphere. 2007; 66(10):1922–1928. [PubMed: 16996563]

16. Allan SE, Smith BW, Anderson KA. Impact of the Deepwater Horizon Oil Spill on Bioavailable Polycyclic Aromatic Hydrocarbons in Gulf of Mexico Coastal Waters. Environmental Science & Technology. 2012; 46(4):2033–2039. [PubMed: 22321043]

17. Baker JE, Eisenreich SJ. Concentrations and fluxes of polycyclic aromatic hydrocarbons and polychlorinated biphenyls across the air-water interface of Lake Superior. Environmental Science & Technology. 1990; 24(3):342–352.

18. Bamford HA, Offenberg JH, Larsen RK, Ko FC, Baker JE. Diffusive exchange of polycyclic aromatic hydrocarbons across the air-water interface of the Patapsco River, an urbanized subestuary of the Chesapeake Bay. Environmental Science & Technology. 1999; 33(13):2138–2144.

19. Fang MD, Lee CL, Jiang JJ, Ko FC, Baker JE. Diffusive exchange of PAHs across the air–water interface of the Kaohsiung Harbor lagoon, Taiwan. Journal of Environmental Management. 2012; 110:179–187. [PubMed: 22789653]

20. Gustafson KE, Dickhut RM. Distribution of polycyclic aromatic hydrocarbons in southern Chesapeake Bay surface water: evaluation of three methods for determining freely dissolved water concentrations. Environmental Toxicology and Chemistry. 1997; 16(3):452–461.

21. Prest H, Jacobson L, Huckins J. Passive sampling of water and coastal air via semipermeable membrane devices. Chemosphere. 1995; 30(7):1351–1361.

22. Lohmann R, Dapsis M, Morgan EJ, Dekany V, Luey PJ. Determining Air– Water Exchange, Spatial and Temporal Trends of Freely Dissolved PAHs in an Urban Estuary Using Passive Polyethylene Samplers. Environmental Science & Technology. 2011; 45(7):2655–2662. [PubMed: 21351793]

23. McDonough CA, Khairy MA, Muir DC, Lohmann R. The significance of population centers as sources of gaseous and dissolved PAHs in the lower Great Lakes. Environmental Science & Technology. 2014; 48(14):7789–7797. [PubMed: 24918966]

24. Lohmann R, Klanova J, Kukucka P, Yonis S, Bollinger K. Concentrations, Fluxes, and Residence Time of PBDEs Across the Tropical Atlantic Ocean. Environmental Science & Technology. 2013; 47(24):13967–13975. [PubMed: 24224767]

25. Lohmann R, Klanova J, Pribylova P, Liskova H, Yonis S, Bollinger K. PAHs on a west-to-east transect across the tropical Atlantic Ocean. Environmental Science & Technology. 2013; 47(6): 2570–2578. [PubMed: 23402581]

26. Ramseur, JL. Deepwater Horizon oil spill: the fate of the oil. Congressional Research Service, Library of Congress; 2010.

27. Tidwell LG, Allan SE, O'Connell SG, Hobbie KA, Smith BW, Anderson KA. Polycyclic Aromatic Hydrocarbon (PAH) and Oxygenated PAH (OPAH) Air–Water Exchange during the Deepwater Horizon Oil Spill. Environmental Science & Technology. 2015; 49(1):141–149. [PubMed: 25412353]

28. Tidwell LG, Allan SE, O'Connell SG, Hobbie KA, Smith BW, Anderson KA. Retraction of "PAH and OPAH Air-Water Exchange during the Deepwater Horizon Oil Spill" due to calculation error. Environmental Science & Technology. 2016 Submitted.

29. Bartkow ME, Jones KC, Kennedy KE, Holling N, Hawker DW, Müller JF. Evaluation of performance reference compounds in polyethylene-based passive air samplers. Environmental Pollution. 2006; 144(2):365–370. [PubMed: 16631287]

30. Booij K, Smedes F, van Weerlee EM. Spiking of performance reference compounds in low density polyethylene and silicone passive water samplers. Chemosphere. 2002; 46(8):1157–1161. [PubMed: 11951981]

31. Huckins JN, Petty JD, Lebo JA, Almeida FV, Booij K, Alvarez DA, Cranor WL, Clark RC, Mogensen BB. Development of the permeability/performance reference compound approach for in situ calibration of semipermeable membrane devices. Environmental Science & Technology. 2002; 36(1):85–91. [PubMed: 11811495]

32. Söderström HS, Bergqvist PA. Passive air sampling using semipermeable membrane devices at different wind-speeds in situ calibrated by performance reference compounds. Environmental Science & Technology. 2004; 38(18):4828–4834. [PubMed: 15487792]

33. Anderson K, Sethajintanin D, Sower G, Quarles L. Field trial and modeling of uptake rates of in situ lipid-free polyethylene membrane passive sampler. Environmental Science & Technology. 2008; 42(12):4486–4493. [PubMed: 18605575]

34. O'Connell SG, McCartney MA, Paulik LB, Allan SE, Tidwell LG, Wilson G, Anderson KA. Improvements in pollutant monitoring: Optimizing silicone for co-deployment with polyethylene passive sampling devices. Environmental Pollution. 2014; 193:71–78. [PubMed: 25009960]

35. O'Connell SG, Haigh T, Wilson G, Anderson KA. An analytical investigation of 24 oxygenated-PAHs (OPAHs) using liquid and gas chromatography–mass spectrometry. Analytical and bioanalytical chemistry. 2013:1–12. [PubMed: 23180075]

36. Bartkow ME, Huckins JN, Müller JF. Field-based evaluation of semipermeable membrane devices (SPMDs) as passive air samplers of polyaromatic hydrocarbons (PAHs). Atmospheric Environment. 2004; 38(35):5983–5990.

37. NOAA. NOAA. 2013. http://tidesandcurrents.noaa.gov/station_retrieve.shtml?type=Meteorological%20Observations

38. [02/10/14] G.S.I.Environmental Chemical Properties Data Base. http://www.gsi-net.com/en/publications/gsi-chemical-database.html

39. Johnson M. A numerical scheme to calculate temperature and salinity dependent air-water transfer velocities for any gas. Ocean Sci. 2010; 6(4):913–932.

40. Matzke MM, Allan SE, Anderson KA, Waters KM. An approach for calculating a confidence interval from a single aquatic sample for monitoring hydrophobic organic contaminants. Environmental Toxicology and Chemistry. 2012; 31(12):2888–2892. [PubMed: 22997050]

41. Lehr B, NRISTOL S, Possolo A. Oil Budget Calculator—Deepwater Horizon, technical documentation: a report to the National Incident Command. Coastal Response Res Cent. 2010

42. Leifer I, Lehr WJ, Simecek-Beatty D, Bradley E, Clark R, Dennison P, Hu Y, Matheson S, Jones CE, Holt B. State of the art satellite and airborne marine oil spill remote sensing: Application to the BP Deepwater Horizon oil spill. Remote Sensing of Environment. 2012; 124:185–209.

43. Middlebrook AM, Murphy DM, Ahmadov R, Atlas EL, Bahreini R, Blake DR, Brioude J, de Gouw JA, Fehsenfeld FC, Frost GJ. Air quality implications of the Deepwater Horizon oil spill. Proceedings of the National Academy of Sciences. 2011

44. Allen, AA.; Jaeger, D.; Mabile, NJ.; Costanzo, D. The use of controlled burning during the Gulf of Mexico Deepwater Horizon MC-252 oil spill response. International Oil Spill Conference Proceedings (IOSC), American Petroleum Institute; 2011. p abs194

45. Brubaker WW, Hites RA. OH reaction kinetics of polycyclic aromatic hydrocarbons and polychlorinated dibenzo-p-dioxins and dibenzofurans. The Journal of Physical Chemistry A. 1998; 102(6):915–921.

46. Jones KC, De Voogt P. Persistent organic pollutants (POPs): state of the science. Environmental Pollution. 1999; 100(1):209–221. [PubMed: 15093119]

47. Terzi E, Samara C. Gas-particle partitioning of polycyclic aromatic hydrocarbons in urban, adjacent coastal, and continental background sites of western Greece. Environmental Science & Technology. 2004; 38(19):4973–4978. [PubMed: 15506188]

48. Ravindra K, Bencs L, Wauters E, De Hoog J, Deutsch F, Roekens E, Bleux N, Berghmans P, Van Grieken R. Seasonal and site-specific variation in vapour and aerosol phase PAHs over Flanders (Belgium) and their relation with anthropogenic activities. Atmospheric Environment. 2006; 40(4):771–785.

49. Khairy MA, Lohmann R. Field validation of polyethylene passive air samplers for parent and alkylated PAHs in Alexandria, Egypt. Environmental Science & Technology. 2012; 46(7):3990–3998. [PubMed: 22397460]

50. He J, Balasubramanian R. The exchange of SVOCs across the air-sea interface in Singapore's coastal environment. Atmos Chem Phys Discuss. 2009; 9:13235–13269.

51. Blumer M, Youngblood W. Polycyclic aromatic hydrocarbons in soils and recent sediments. Science. 1975; 188(4183):53–55. [PubMed: 17760164]

52. Zhang W, Zhang S, Wan C, Yue D, Ye Y, Wang X. Source diagnostics of polycyclic aromatic hydrocarbons in urban road runoff, dust, rain and canopy throughfall. Environmental Pollution. 2008; 153(3):594–601. [PubMed: 17949873]

53. Aeppli C, Carmichael CA, Nelson RK, Lemkau KL, Graham WM, Redmond MC, Valentine DL, Reddy CM. Oil Weathering after the Deepwater Horizon Disaster Led to the Formation of Oxygenated Residues. Environmental Science and Technology-Columbus. 2012; 46(16):8799.

54. Albinet A, Leoz-Garziandia E, Budzinski H, ViIlenave E. Polycyclic aromatic hydrocarbons (PAHs), nitrated PAHs and oxygened PAHs in ambient air of the Marseilles area (South of France): Concentrations and sources. Science of The Total Environment. 2007; 384(1-3):280–292. [PubMed: 17590415]

55. Wilson NK, McCurdy TR, Chuang JC. Concentrations and phase distributions of nitrated and oxygenated polycyclic aromatic hydrocarbons in ambient air. Atmospheric Environment. 1995; 29(19):2575–2584.

56. Albaigés J, Bayona JM, Fernandez P, Grimalt J, Rosell A, Simó R. Vapor-particle partitioning of hydrocarbons in Western Mediterranean urban and marine atmospheres. Microchimica Acta. 1991; 104(1):13–27.

57. Cincinelli A, Bubba MD, Martellini T, Gambaro A, Lepri L. Gas-particle concentration and distribution of *n*-alkanes and polycyclic aromatic hydrocarbons in the atmosphere of Prato (Italy). Chemosphere. 2007; 68(3):472–478. [PubMed: 17307224]

58. Eiguren-Fernandez A, Avol EL, Thurairatnam S, Hakami M, Froines JR, Miguel AH. Seasonal influence on vapor-and particle-phase polycyclic aromatic hydrocarbon concentrations in school communities located in Southern California. Aerosol science and technology. 2007; 41(4):438–446.
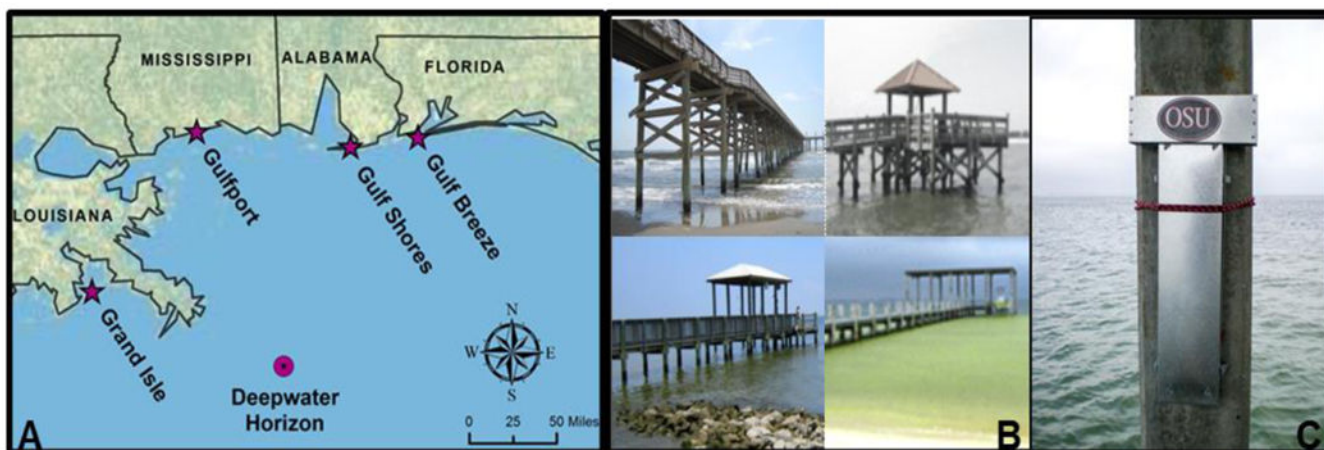
Figure 1.
A.) Sampling locations along the Gulf of Mexico. B.) Samplers deployed off piers at each sampling site. C.) Air sampling cage affixed to pier in Gulf Breeze, FL.
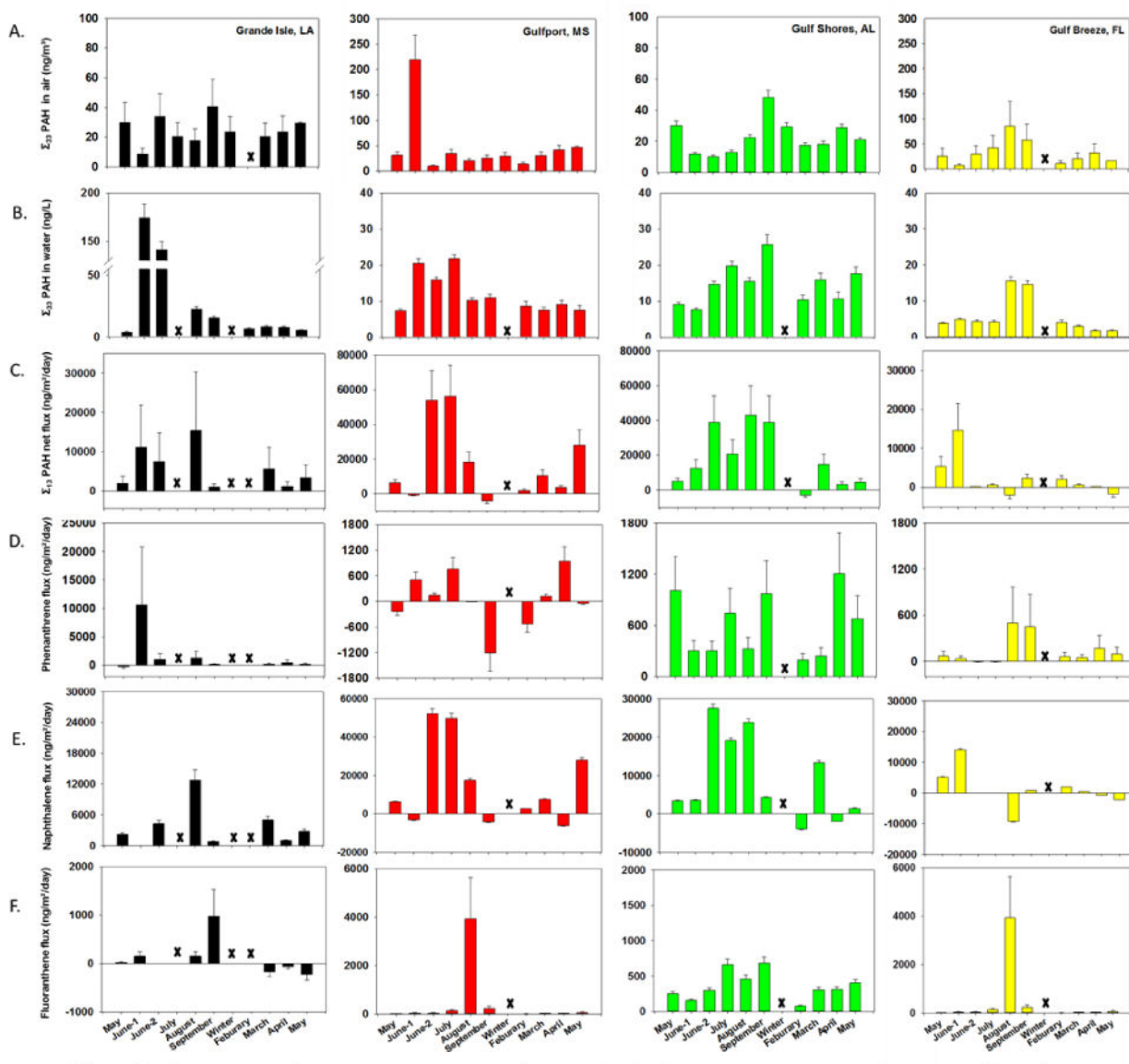
Figure 2.
A.)Σ_{33} PAH vapor phase concentrations in air. B.) Σ_{33} PAH dissolved concentrations in water.[16] C.) Σ_{13} PAH net flux D.) Phenanthrene flux. E.) Naphthalene flux. F.) Fluoranthene flux. Error bars represent the calculated 95% confidence interval based on pooled variance from a replication study.
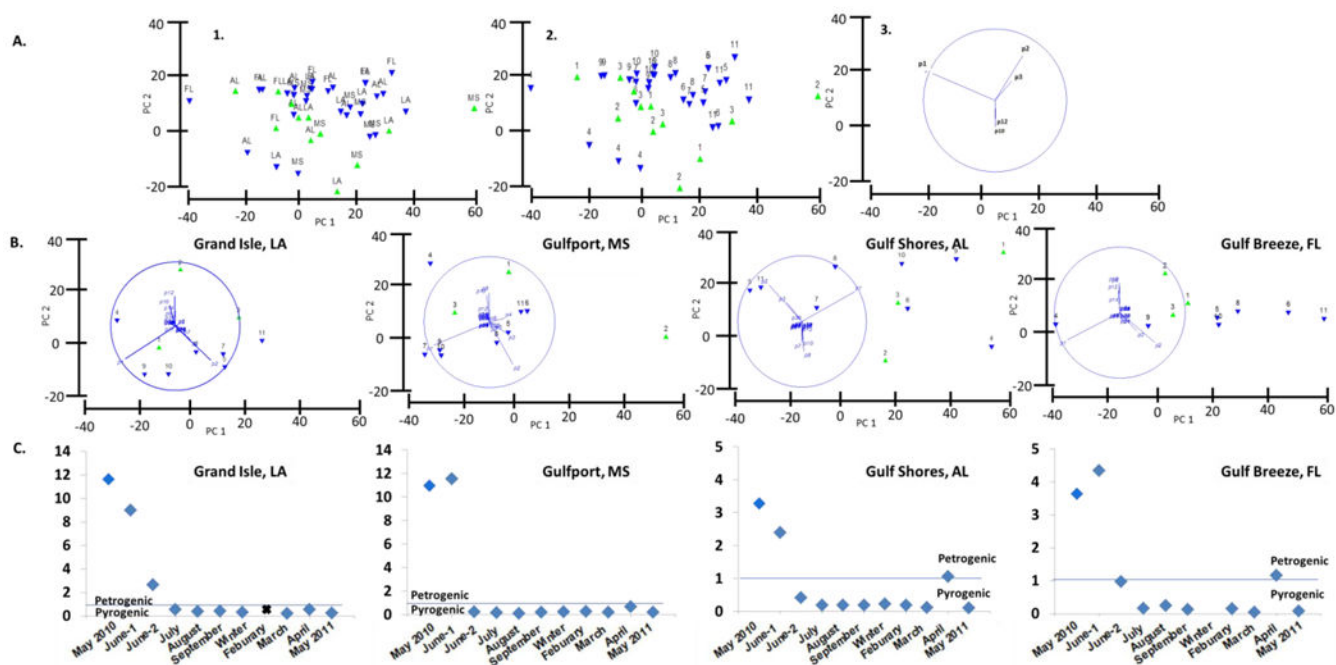
Figure 3.
A.) Principal component analysis (PCA) plots representing all sampling events. Green and blue triangles represent samples prior to, and after the well head was capped respectively. A1 is labeled by state, and A2 is labeled by events numbered #1 through 11 (representing May 2010 to May 2011), and A3 are PAH vectors (p1= naphthalene, p2= 1-methylnaphthalene, p3= 2-methylnaphthalene, p10= phenanthrene, p12=2-methylphenanthrene). B.) Individual state PCA plots. C.) Ratio of 2-3 ring/4-6 ring PAHs for each site during each sampling event.
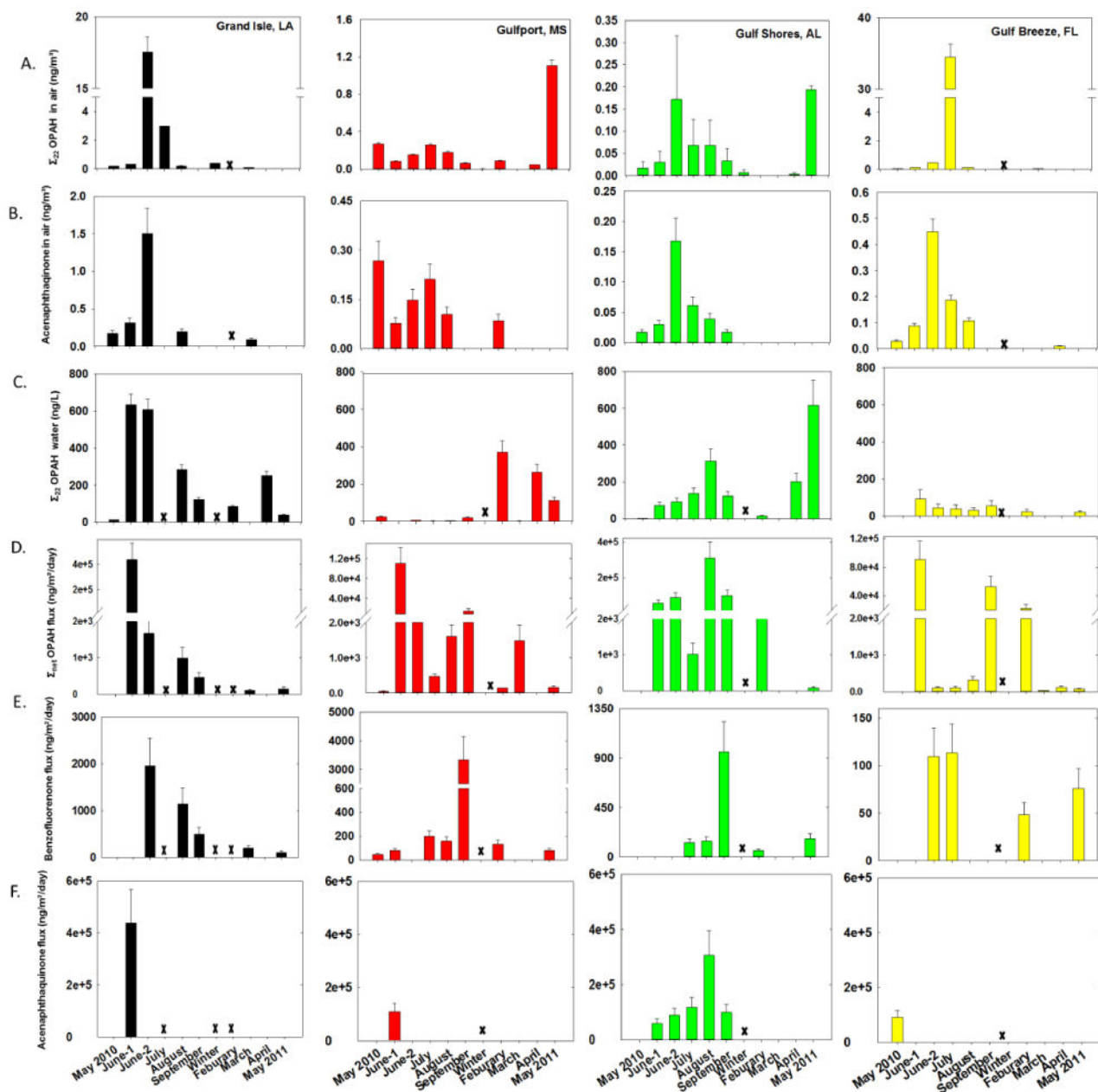
Figure 4.
A.) Σ_{22} OPAH vapor phase concentrations in air. B.) Acenaphthenequinone vapor phase concentrations in air. C.) Σ_{22} OPAH dissolved concentrations in water. D.) Σ_7 OPAH net flux E.) Benzofluorenone flux. F.) Acenaphthenequinone flux. Error bars represent the calculated 95% confidence interval based on pooled variance from a replication study.